Published in final edited form as:
Neurobiol Dis. 2014 February ; 62: . doi:10.1016/j.nbd.2013.08.018.

Loss of cholecystokinin-containing terminals in temporal lobe epilepsy

Chengsan Sun[1,2,*], **Jianli Sun**[1,*], **Alev Erisir**[2], and **Jaideep Kapur**[1]

[1]Department of Neurology, Box 800394, University of Virginia, Health Sciences Center, Charlottesville, VA 22908

[2]Department of Psychology, PO Box 400400, University of Virginia, Charlottesville, VA, 22904

Abstract

Altered GABA-mediated inhibition is proposed to play a role in the pathogenesis of epilepsy. Previous studies have demonstrated a loss of somatostatin-containing GABAergic interneurons innervating granule cells in epileptic animals. However, the reorganization of synapses between interneurons and granule cells has not been investigated. We studied synapse organization in an animal model of temporal lobe epilepsy (TLE) using continuous hippocampal stimulation. The distribution of axon terminals and inhibitory synapses on granule cell dendrites was studied using a combination of immunohistochemistry and pre-embedding electron microscopy techniques. A whole-cell patch-clamp technique was applied to study the functional changes in GABAergic input from different interneurons. In epileptic animals, the density of cholecystokinin (CCK)-immunoreactive (IR) fibers and $\alpha 2$ subunit containing $GABA_A$ receptors in the inner molecular layer of the dentate gyrus was reduced. Quantitative immuno-electron microscopy study revealed that the ratio of CCK-containing symmetric synapses to the total symmetric synapses was reduced. The frequency of GABAergic synaptic currents (sIPSC) was decreased and their amplitude was increased. The inhibitory effect of the activation of cannabinoid 1(CB1) receptors was also reduced in epileptic animals. Isolation of CCK- and parvalbumin (PV)-containing GABAergic inputs by N- and P/Q-type calcium channel blockers respectively suggested that GABA release from CCK-containing interneurons was selectively reduced in epileptic rats. This study found that there was a loss of CCK-containing GABAergic synapses to granule cells both morphologically and functionally. These studies add to our understanding of the mechanisms that contribute to altering GABAergic inhibition of granule cells in TLE.

Keywords

GABAergic interneuron; cholecystokinin-containing symmetric synapses; dentate gyrus; spontaneous inhibitory postsynaptic currents; epilepsy

Corresponding author: Jaideep Kapur, MD, PhD, Department of Neurology & Neuroscience, Box 800394, University of Virginia-HSC, Charlottesville, VA 22908, Phone: 434-924-5312, Fax: 434-982-1726, jk8t@virginia.edu.
*Equal contribution

Introduction

In animal models of temporal lobe epilepsy (TLE), GABAergic inhibition is altered (Joshi S & Kapur J, 2012). Inhibitory interneurons in the hippocampus play a crucial role in generating inhibitory effects (Hefft & Jonas P., 2005). GABAergic terminals are abundant throughout the dentate gyrus, with the highest densities in the outer third of the molecular layer and slightly lower densities in the inner two-thirds of this layer (Houser, 2007). The cell bodies and proximal dendrites of dentate granule cells are innervated by a dense plexus of GABAergic terminals arising from cholecystokinin (CCK) and parvalbumin (PV)-containing basket cells; distal dendrites are innervated by somatostatin (SOM)-positive terminals (Houser, 2007). Some somatostatin-containing interneurons are lost in animal models of TLE (Best et al., 1993; Houser, 1991; Buckmaster & Dudek, 1997; Sloviter, 1987; Sun et al., 2007a). Similar findings are reported in TLE patients (de Lanerolle et al., 1989; Maglóczky et al., 2000; Mathern et al., 1996). However, it is unknown whether CCK, PV, or SOM terminals in the hippocampal dentate gyrus are reorganized in epileptic animals.

PV and CCK basket cells are two major inhibitory interneurons that connect at perisomatic and proximal dendritic inhibitory synapses in the dentate gyrus. Their terminals contain the GABA synthetic enzyme glutamic acid decarboxylase (GAD) and form symmetric inhibitory contacts primarily on the cell bodies and shafts of apical dendrites of the granule cells (Kosaka et al., 1984). It has been proposed that PV interneurons operate as clocks for cortical network oscillations, whereas CCK interneurons function as a plastic fine-tuning device in the hippocampus (Freund & Katona, 2007). CCK basket cells influence their target cells by activating α2 subunit containing $GABA_A$ receptors (Nyíri G. et al., 2001). The α2 subunit containing $GABA_A$ receptors were absent or expressed at very low levels at synapses formed by PV interneurons (Freund & Katona, 2007). Cannabinoid receptor type I (CB1) and M1/M3 acetylcholine receptors are expressed in CCK- but not PV-containing terminals (Freund & Katona, 2007; Katona et al., 1999). CCK-containing basket cells express N-type calcium channels, whereas PV-containing cells express P/Q-type calcium channels (Hefft & Jonas P., 2005; Poncer et al., 1997; Wilson et al., 2001). These specific biological markers can be used to distinguish these two types of interneurons.

The present study investigated the IR distribution of SOM, PV, and CCK terminals, as well as the α2 subunit of $GABA_A$ receptor in the dentate gyrus using fluorescent microscopy. There was reduced staining of CCK and the α2 subunit in the inner molecular layer in epileptic animals. Pre-embedding electron microscopy experiments demonstrated a reduction of CCK-positive symmetric synapses in epileptic animals. Furthermore, postsynaptic CCK-containing GABAergic currents recorded from dentate granule cells demonstrated reduced perisomatic inhibition in epileptic animals. This suggested that loss of CCK-containing GABA interneuron terminals and synapses in the dentate gyrus may cause impairment of inhibitory function in the neuron circuit, which then leads to seizure discharge in patients.

Materials and methods

Animal model

Animals were handled according to AALAC Animal Care and Use Guidelines and a protocol approved by the University of Virginia Animal Care and Use Committee. Status epilepticus (SE) was induced in adult male Sprague-Dawley rats (2–4 month old) using the previously described continuous hippocampal stimulation method (Lothman et al., 1989). Briefly, bipolar electrode was stereotactically implanted in the hippocampus (AP −3.6; ML 4.9; DV −5.0 to dura). Stimulations were delivered 1–2 weeks after surgery. Approximately

4–6 weeks after stimulation, animals developed spontaneous limbic seizures, which were detected by continuous EEG monitoring and direct observation of a behavioral seizure (Bertram et al., 1997). Animals with 3 month recurrent spontaneous seizures and age-matched controls were used for this study.

Immunohistochemistry for neuropeptide-IR interneurons

The procedures for tissue preparation were described in detail previously (Sun et al., 2004). Briefly, animals were anesthetized with an overdose of pentobarbitone sodium and perfused through the ascending aorta with 50–100 ml of 0.9 % NaCl followed by 350–450 ml of 4 % paraformaldehyde in 0.1 M phosphate buffer (PB, pH 7.4). The brains were removed and postfixed in the same fixative for 2 hours (hr) at 4 °C. After overnight incubation in a solution of 30 % sucrose in 0.1 M PB for cryoprotection, the brains were separated and blocked as previously described (Sun et al., 2007a). The brains were frozen by immersion in −70 °C isopentane and the ventral hippocampus was sectioned (40 μm thick) horizontally.

The sections were processed for free floating immunohistochemistry, as described in detail previously (Sun et al., 2004; Sun et al., 2007a). Following 3 washes in 0.1 M PB, the sections were incubated with blocking solution containing 5 % normal goat serum, 2 % bovine serum albumin (BSA; Jackson Immunoresearch Laboratories, Inc. West Grove, PA), and 0.1 % Triton X-100 in 0.1 M phosphate-buffered saline (PBS, pH 7.4) for 1 hr. The tissue sections were placed on a shaker and incubated with the primary antibodies at 4 °C for 72 hr, and then incubated in the dark with goat anti-rabbit or goat anti-mouse secondary antibodies conjugated with Alexa Fluor 488 or 594 (Molecular Probes, Eugene, OR, 5 μg/ml) for 1 hr at room temperature. All antibodies were diluted with a solution containing 1 % BSA in 0.1 M PBS. The sections were quickly rinsed 3 times and followed by 6 washes after the incubation with primary and secondary antibodies. Then, sections were mounted on a slide with Gel/Mount (Foster City, CA) and covered with a coverslip. After air-drying for approximately1 hr, the edges of the coverslips were sealed with clear nail polish. We have characterized all antibodies (Sun et al., 2007a; Mangan et al., 2005).

Images of tissue sections were captured on a CoolSnap cf CCD camera (Roper Scientific Photometrics) mounted on an Eclipse TE200 microscope (Nikon) equipped with a mercury lamp and filters for detecting fluorescence, driven by Metamorph imaging software (Universal Imaging Corp., Downington, PA). Three 40 μm squares per section were randomly chosen to measure optical density. Data were analyzed using Prism 4.0 software (GraphPad Software, Inc. San Diego, CA). Unless specified otherwise, all values are reported as the mean ± standard error of the mean (SEM), and an unpaired Student *t*- test was used to determine significance.

Pre-embedding electron microscopy

Pre-embedding electron microscopy study of CCK-positive terminals was performed following a previously published protocol (Sun et al., 2007a). Animals were transcardially perfused with Tyrode solution (Heck et al., 2002). A fixative consisting of 4 % paraformaldehyde and 0.1 % glutaraldehyde (or 2 % paraformaldehyde and 2 % glutaraldehyde for the synaptic profile study) in 0.1 M PB was perfused until the effluent was clear. The brains were post-fixed in 4 % paraformaldehyde for 2 hr at 4 °C, and sliced in PB on a vibratome at a thickness of 60 μm. Sections were treated with 0.1 % $NaBH_4$ at room temperature for 30 minutes, and then rinsed with PB. The sections were rinsed and treated in 1 % bovine serum albumin (BSA) in PBS for 30 min. They were then incubated in a 1:50 dilution of monoclonal mouse anti-CCK antibody (Abcam Inc., Cambridge, MA) in PBS with 1 % BSA and 0.05 % sodium azide for 3 days at room temperature. Then, sections were rinsed and incubated in a biotinylated goat anti-mouse secondary antibody (Vector

Laboratories, Burlingame, CA) for 2 hr, followed by a 2 hr incubation in HRP-conjugated avidin-biotin complex (ABC; Vector Laboratories). Immunoreactivity was visualized using diaminobenzidine (DAB, 0.03 %) and H_2O_2 (0.001 %). Deletion of the primary antibody eliminated all of the specific staining discernible at the electron microscopy level.

The sections were put in 1% osmium tetroxide in PB for 1 hour, dehydrated, and flat-embedded in Epon 812 resin between two sheets of Aclar film (Electron Microscopy Sciences, Fort Washington, PA). After resin polymerization, a small area including the molecular layer, granule cell layer, and part of the hilus was dissected from the ventral hippocampus and mounted on capsules. Ultrathin sections at the interface of tissue and resin were collected and stained with uranyl acetate and lead citrate. Grids were examined on a Jeol JEM 1010 microscope, and images were captured by a 16 megapixel SIA-12C (sia-cam.com) digital camera coupled with MaxIm DL CCD software (Diffraction Limited, Ottawa, Canada).

For quantitative electron microscopy analysis with systematic sweeps, each synapse was located, and its length was measured with Image-ProPlus 4.5 software (Media Cybernetics, Silver Spring, MD). The type of synaptic contact (symmetric or asymmetric) and the type of postsynaptic element (dendrite shaft, spine, or soma) were evaluated by the criteria detailed in a previous study (Sun et al., 2007b). The length of the synapse was measured along the parallel-aligned plasma membranes. The areal density of synapses (N_A indicates the number of synapses per area) was calculated and used to find the volumetric density of synapses ($N_V = N_A$/average synaptic length).

Whole-cell electrophysiological recording

Whole-cell patch-clamp recordings of GABA receptor currents (sIPSCs) from dentate granule cells (DGCs) in hippocampal slices were performed as previously described (Sun et al., 2007b). Adult male Sprague–Dawley rats were anesthetized with isoflurane and decapitated, brains were quickly removed, and then brains were sectioned with a 300 μm thickness using a Leica VT 1200 slicer (Leica Microsystems, Wetzlar, Germany) in ice cold oxygenated slicing solution. The solution contained the following (in mM): 120 sucrose, 65.5 NaCl, 2 KCl, 1.1 KH_2PO_4, 25 $NaHCO_3$, 10 D-glucose, 1 $CaCl_2$, and 5 $MgSO_4$. The slices were then incubated at 32 °C for at least one hour in oxygenated ACSF containing the following (in mM): 127 NaCl, 2 KCl, 1.1 KH_2PO_4, 25.7 $NaHCO_3$, 10 D-glucose, 2 $CaCl_2$, and 1.5 $MgSO_4$; osmolality was 290–300 mOsm in the chamber. Slices were then transferred to the recording chamber on the stage of an Olympus Optical BX51 microscope (Olympus, Tokyo).

Whole-cell patch-clamp recordings were performed under infrared differential interference contrast microscopy (Olympus) with a 40× water-immersion objective to visually identify dentate granule cells. Slices were continuously superfused with ACSF solution saturated with 95 % O_2– 5 % CO_2 at room temperature. Patch electrodes (final resistances, 3–5 MΩ) were pulled from borosilicate glass (Sutter Instruments, Novato, CA) on a horizontal Flaming-Brown microelectrode puller (Model P-97, Sutter Instruments). Electrode tips were filled with a filtered internal recording solution consisting of (in mM) 153.3 CsCl, 1 $MgCl_2$, 10 HEPES, 5 EGTA, and 3 ATP Mg^{2+} salt, pH adjusted to 7.3 with CsOH (osmolality, 305 mOsm). Neurons were voltage clamped to −65 mV with a PC-505B amplifier (Warner Instruments, Hamden, CT). Electrode capacitance was electronically compensated. Access resistance was continuously monitored, and if the series resistance increased by 20 % at any time, then the recording was terminated. Currents were filtered at 2 k Hz, digitized by a Digidata 1322 digitizer (Molecular Devices, Sunnyvale, CA), and acquired with Clampex 10.2 software (Molecular Devices). Spontaneous inhibitory postsynaptic currents (sIPSC) were recorded from DGCs after blocking AMPA and NMDA receptors with 6-cyano-7-

nitroquinoxalene-2,3-dione (CNQX, 20 μM) and 2-amino-5-phosphonovaleric acid (APV, 50 μM), respectively.

The off-line digitized data were analyzed with MiniAnalysis (Synaptosoft, Decatur, GA) and Clampfit 10.2 (Molecular Devices). To detect sIPSCs, a detection threshold was set at three times root mean square (RMS) of baseline noise. Each detected event in the 25–45 min recording was visually inspected to remove false detections. The frequency and peak amplitude of sIPSC were analyzed for individual neurons. The Kolmogorov-Smirnov (K–S) test was used to compare amplitudes and inter-event intervals for continuously recorded IPSCs. Event frequency and amplitudes were compared using Student's *t*-test. Drug application data were analyzed using a paired *t*-test. The *P* values represent the results of Student's *t*-test analysis, with $p < 0.05$ indicating the level of significance. Data values were expressed as the means ± SEM unless noted otherwise.

Results

Distribution of SOM, PV, and CCK immunoreactivity in the molecular layer of the dentate gyrus

CCK-, PV- and SOM-containing terminals were found in different strata of the molecular layer of the hippocampal dentate gyrus. SOM immunoreactivity (IR) was mainly distributed in the outer molecular layer (Fig. 1A), and similar distribution was found in epileptic animals (Fig. 1B). PV-IR was mainly distributed in the dentate granule cell layer and formed a dense plexus around the granule cells (Fig. 1C), and there was no apparent difference in epileptic animals (Fig. 1D). CCK-IR was located in the inner and middle molecular layer in control animals (Fig. 1E), and it appeared less intense in the inner molecular layer of epileptic animals (Fig. 1F).

Reduced CCK and α2 immunoreactivity in the inner molecular layer of the dentate gyrus in TLE

The distribution of CCK in the inner molecular layer of the dentate gurus was studied further using higher resolution images. In control animals, CCK-IR was observed mainly in the inner molecular layer, with less intense staining in the middle molecular layer, granule cell layer, and the hilar border of the granule cell layer (Fig. 2A). In epileptic animals, the distribution of CCK-IR in the molecular layer was distributed differently. The intensity of CCK-IR in epileptic animals appeared decreased in the inner molecular layer and slightly increased in the middle molecular layer (Fig. 2B). Quantitative analysis of the optical density (OD) demonstrated that the ratio of the inner molecular layer OD to middle molecular layer OD was lower in epileptic animals (0.86 ± 0.02, n = 27 sections, 4 animals) compared with that in control animals (1.28 ± 0.03, n = 26 sections, 4 animals, $p < 0.001$).

CCK-containing GABAergic interneurons influence their target by acting via $GABA_A$ receptors enriched in α2 subunits (Nyíri G. et al., 2001). To investigate the postsynaptic reorganization corresponding to the presynaptic CCK reorganization, the α2 subunit of $GABA_A$ receptor in DGCs was investigated. In control animals, the α2-IR staining was mainly distributed in the inner molecular layer, and it was also found in the middle and outer molecular layers, as well as the dentate granule cell layer (Fig. 2C). However, in epileptic animals (Fig. 2D) α2 subunit-IR staining was decreased in the inner molecular layer compared with controls (Fig. 2C). The α2 subunit-IR OD ratio of the inner molecular layer to the middle molecular layer was lower in epileptic animals (0.83 ± 0.02, 38 sections, 5 animals) compared with that in control animals (1.11 ± 0.02, 38 sections, 5 animals, $p < 0.05$). The similar reorganization of CCK-IR and α2-IR staining in the inner molecular layer in epileptic animals was demonstrated using merged images (Fig. 2E,F). The linescan

histogram of profile mapping images demonstrated that the gray levels of CCK and α2 subunit staining in the inner molecular layer were reduced in epileptic animals compared with that in control animals (Fig. 2G,H).

In merged images, a similar reduction of CCK and α2 subunit-IR staining in the inner molecular layer was found in epileptic animals, and there was some overlap of CCK- and α2 subunit-IR staining in the inner molecular layer in both control and epileptic animals (Fig. 2E,F). The CCK-IR staining overlapped with the α2 subunit-IR staining and their similar reorganization in epileptic animals suggests that they might represent a specific subset of GABAergic synapses and were altered in chronic epileptic animals.

Reduced CCK symmetric synapses in epileptic animals

Reduced CCK-IR in the inner molecular layer could represent a loss of neuropeptides or a reorganization of terminals. To determine if the reduced CCK-IR staining was associated with a decrease in the number of CCK-IR symmetric synapses, we examined the pre-embedding CCK-IR in the inner molecular layer of the dentate gyrus using electron microscopy. Dark CCK-IR was found predominately in terminals, and fewer CCK-IR profiles appeared to be present in epileptic animals (Fig. 3B,D) compared with control animals (Fig. 3A,C). CCK-IR terminals made symmetric synapses with proximal dendrites of granule cells in the dentate gyrus (Fig. 3A–D), and the CCK-IR dendrites were restricted to proximal segments (data not shown) in control animals. These were similar to those described in previous studies (Leranth & Frotscher, 1986). Furthermore, the number of CCK-positive symmetric synapses and total symmetric synapses were counted in the images captured from three epileptic animals and three controls. There was a significant difference in the number of CCK-containing symmetric synapses and total symmetric synapses in control (120, 193) and epileptic animals (71, 165, Fisher's exact test, $p < 0.05$). The ratio of the number of CCK-IR symmetric synapses to that of the total symmetric synapses in epileptic animals (0.4303) was lower than that in controls (0.6218). In summary, the CCK-containing symmetric synapses were diminished in the inner molecular layer of epileptic animals, which suggested that the CCK-containing interneuron-mediated inhibition was decreased in epileptic animals.

The volume density of symmetric synapses in the inner molecular layer of the dentate gyrus in TLE animals was unaltered

To determine whether the reduction in CCK-positive symmetric synapses was associated with a decrease in the number of total symmetric synapses in the inner molecular layer, we measured the average volumetric synaptic density (N_v) in the neuropil of the inner molecular layer from control and epileptic animals. CCK-positive symmetric synapses are a main component of total symmetric synapses in this layer, and the total symmetric synapses might be reduced proportionally due to the decreased CCK-positive symmetric synapses. Symmetric synapses made by terminals and dendritic shafts in the inner molecular layer were found in control (Fig. 4A,B) and epileptic animals (Fig. 4C–E), and asymmetric synapses made by terminals and spines were also found in both groups. In epileptic animals, some mossy fibers were found in the inner molecular layer (Fig. 4D), which were identified by their large size (>1 μm), high concentrations of clear round vesicles, forming distinct asymmetric synapses, and their irregular shapes (Commons & Milner, 1997).

The synaptic profiles including symmetric and asymmetric synapses in the inner molecular layer of the dentate gyrus were analyzed from control and epileptic animals with Image plus 4.5 as detailed in the methods section. We examined a total of 1606 μm^2 and 1590 μm^2 in the inner molecular layer from 3 control animals and 3 epileptic animals, respectively. The average volumetric synaptic density (N_V) of total synapses in the inner molecular layer in

control animals (N_v = 14.72 ± 0.97, 10^8 per mm^3, 3 animals) was similar to that in epileptic animals (N_v = 13.38 ± 0.90, 10^8 per mm^3, 3 animals, unpaired t test, $p > 0.05$, Fig. 5A). The N_v of symmetric synapses in the inner molecular layer in control animals (1.01 ± 0.24) was not different from that in epileptic animals (1.33 ± 0.15, $p > 0.05$, Fig. 5B), and our result in control animals was similar to that of a previous study that observed the same region (Halasy & Somogyi P., 1993). The N_v of asymmetric synapses in the inner molecular layer had a tendency to decrease, but there was no significant difference between control (13.97 ± 0.97) and epileptic animals (12.03 ± 1.02, $p > 0.05$, Fig. 5B).

In summary, these studies revealed that the total number of symmetric synapses was not changed in epileptic animals, but the density of CCK-containing symmetric synapses was diminished. The functional effect of reduced CCK-containing symmetric synapses was then determined.

GABAergic synaptic currents were changed in TLE animals

We compared the frequency and amplitude of sIPSCs in dentate granule cells (DGCs) between epileptic and naïve rats. The mean frequency of sIPSC was not different between the two groups of rats (naïve: 11.37 ± 1.64 Hz, n = 35; epileptic: 11.04 ± 0.79 Hz, n = 29; $p = 0.43$); however, the amplitude was increased in epileptic rats (naïve: 87.99 ± 5.62 pA, n = 35; epileptic: 112.92 ± 5.79 pA, n = 29; $p < 0.01$). Histogram distribution analysis showed that the sIPSC frequency had more peaks in epileptic rats, and the biggest peak was left-shifted from the naïve rats (Fig. 6A). The K–S test on a cumulative frequency plot demonstrated that the cumulative distribution of sIPSC frequency was significantly left-shifted in epileptic rats (d: 0.36, $p < 0.05$, Fig. 6B). The histogram distribution (Fig. 6C) and cumulative distribution (Fig. 6D) of sIPSC amplitude were significantly right-shifted. This suggested that the frequency of sIPSC was decreased but its amplitude was increased in epileptic rats.

The effect of CB1 activation on GABAergic synaptic transmission to DGCs was reduced in TLE animals

CB1 cannabinoid receptors are selectively expressed in presynaptic CCK-containing terminals, and their activation has inhibitory effects on GABA release. If CCK inputs are reduced as demonstrated by immunohistochemistry and pre-embedding electron microscopy studies, the effect of CB1 agonist on sIPSC frequency should be altered. To test this prediction, the effect of CB1 agonist WIN 55212-2 mesylate [*R*(+)-[2,3-dihydro-5-methyl-3-[(morpholinyl)]pyrrolo[1,2,3-de]-1,4-benzoxazinyl]-(1-naphthalenyl) methanone mesylate] (WIN, 5 μM) on sIPSC was then studied. WIN significantly decreased the frequency of sIPSC in both control (baseline 14.13 ± 1.92 Hz, WIN 8.94 ± 1.65 Hz, n = 7, $p < 0.01$, Fig. 7A) and epileptic animals (baseline 7.61 ± 2.07 Hz, WIN 5.62 ± 1.31 Hz, n = 7, $p < 0.05$, Fig. 7B). WIN also decreased the amplitude of sIPSC in both groups (naïve: baseline 76.71 ± 7.82 pA, WIN 67.05 ± 6.65 pA, n = 7, $p < 0.01$; epileptic: baseline 113.38 ± 15.68 pA, WIN 88.58 ± 7.98 pA, n = 7, $p < 0.05$, Fig 7A,B). WIN significantly right-shifted the cumulative distribution of the inter-event intervals of sIPSC in both groups, but its effect was reduced in epileptic rats (Fig. 7C,E), which suggested that WIN decreased the frequency of sIPSC and had a less effect in epileptic rats. WIN also left-shifted the cumulative distribution of the sIPSC amplitude in both groups, and there was no difference between the two groups (Fig. 7D,F), which suggested that WIN decreased the amplitude of sIPSC. Quantification of the effect of WIN on the frequency and amplitude sIPSC showed that WIN had a reduced effect on the frequency (naïve: 60.95 ± 4.21 % of baseline, epileptic: 83.94 ± 7.52 % of baseline, n = 7, $p < 0.05$, Fig. 7G) in epileptic rats, but there was no difference in its effect on amplitude (naïve: 87.83 ± 3.87 % of baseline, epileptic: 83.39 ± 7.60 % of baseline, n = 7, $p = 0.44$, Fig. 7H). These data suggest that the inhibitory

effect of CB1 receptor activation on CCK-containing GABAergic synaptic transmission was reduced in epileptic rats.

The effect of an N-type calcium channel blocker on GABA release was reduced in TLE animals

PV and CCK basket cells are two major inhibitory interneurons that mainly contribute to perisomatic and proximal dendritic inhibitory synapses in the dentate gyrus. PV-containing basket cells express P/Q-type calcium channels, whereas CCK-containing basket cells express N-type calcium channels (Freund & Katona, 2007; Katona et al., 1999). N-type channels trigger synchronous and asynchronous release in CCK interneuron synapses, whereas P/Q-type calcium channels mediate release at PV interneuron synapses (Hefft & Jonas P., 2005). To study those two components separately, we applied an N-type channel blocker, ω-conotoxin GVIA (CTX, 1 μM), and a P/Q-type of calcium channel blocker, ω-agatoxin TK (500 nM), to isolate CCK and PV GABAergic inputs to DGCs.

In naïve rats, CTX decreased the frequency of sIPSC to 50.92 ± 5.10 % (n = 6, $p < 0.01$, Fig. 9A,F), and right-shifted the cumulative distribution of inter-event intervals of sIPSC (Fig. 8B). CTX also decreased the amplitude of sIPSC to 77.36 ± 1.58 % (n = 6, $p < 0.01$, Fig. 8A,G), and left-shifted its cumulative distribution (Fig. 8C). WIN had no further effect when applied after CTX either on the frequency (n = 6, $p = 0.89$, Fig. 8A,B,F) or amplitude (n = 6, $p = 0.17$, Fig. 8A,C,G) of sIPSC. This was consistent with the selective expression of CB1 receptors on CCK basket neuron terminals. As GABA release from CCK-containing terminals was blocked by CTX, it is to be expected that WIN would not have any effect.

In epileptic rats, CTX decreased the frequency of sIPSC to 78.29 ± 7.10 % (n = 6, $p < 0.05$, Fig. 8A,F), and right-shifted the cumulative distribution of inter-event intervals of sIPSC (Fig. 8D). The effect of CTX was significantly attenuated compared with that in naïve rats ($p < 0.05$). CTX did not change the amplitude of sIPSC (n = 6, $p = 0.41$, Fig. 8A,G) or shift its cumulative distribution (Fig. 8E). Similar to the findings in naïve rats, WIN had no further effect after CTX on the frequency (n = 6, $p = 0.33$, Fig. 8A,D,F) or amplitude (n = 6, $p = 0.15$, Fig. 8A,E,G) of sIPSC in epileptic rats. These data suggested that CCK-containing GABAergic inputs to DGCs were reduced in epileptic rats (Table 1).

The effect of a P/Q-type calcium channel blocker on GABA release was relatively increased in TLE animals

The P/Q-type calcium channel blocker ω-agatoxin TK (Agtx, 500 nM) blocked most events of sIPSC in DGCs in both naïve and epileptic rats (Table 2). In naïve rats, Agtx decreased the frequency of sIPSC to 24.30 ± 2.18 % (n = 8, $p < 0.01$, Fig. 9A,G), and right-shifted the cumulative distribution of inter-event intervals of sIPSC (Fig. 9C). Agtx also decreased the amplitude of sIPSC to 67.74 ± 5.07 % (n = 8, $p < 0.01$, Fig. 9A,H), and left-shifted its cumulative distribution (Fig. 9D). WIN decreased the frequency of sIPSC further when applied after Agtx (n = 8, $p < 0.01$, Fig. 9A,G) and shifted its cumulative distribution more to the right (Fig. 9C). WIN had no further effect on the amplitude of sIPSC (n = 8, $p = 0.17$, Fig. 9A,H). This was also consistent with the finding that CB1 receptors are selectively expressed on CCK basket neuron terminals. As Agtx blocked GABA release from PV-containing interneurons, the remaining events represented mostly GABA release from CCK-containing interneurons.

In epileptic rats, Agtx decreased the frequency of sIPSC to 18.97 ± 2.52 % (n = 7, $p < 0.01$, Fig. 9B,G), and right-shifted the cumulative distribution of inter-event intervals of sIPSC (Fig. 9E). Agtx had a stronger effect in epileptic rats than in naïve rats ($p < 0.05$, Fig. 9G). Agtx decreased the amplitude of sIPSC to 71.97 ± 3.86 % (n = 7, $p < 0.01$, Fig. 9B,F) and

left-shifted its cumulative distribution (Fig. 9E). There was no difference in the effect of Agtx on the amplitude of sIPSCs between the two groups of rats ($p = 0.27$, Fig. 9H). WIN decreased the frequency of sIPSC further when applied after Agtx (n = 7, $p < 0.05$, Fig. 9A,G) and shifted its cumulative distribution to the right (Fig. 9C). WIN had no further effect on the amplitude of sIPSC (n = 7, $p = 0.16$, Fig. 9A,H). The effect of WIN on both frequency ($p = 0.14$) and amplitude ($p = 0.14$) were not different between naïve and epileptic rats. These data suggest that the relative PV-containing GABAergic inputs to DGCs were increased in epileptic rats and associated with the reduction of CCK-containing GABAergic inputs.

Discussion

We studied the plasticity of the CCK-containing GABAergic interneurons-DGC synapses in the molecular layer of the dentate gyrus in epileptic animals, and four major findings emerged. First, immunoreactivity labeling of CCK and the α2 subunit of $GABA_A$ receptor were decreased in the inner molecular layer after recurrent spontaneous seizures. Second, the ratio of CCK-positive symmetric synapses versus total symmetric synapses was decreased, but the volumetric synaptic density in the inner molecular layer was unchanged. Third, GABA release from CCK-containing interneurons to DGCs was reduced. Finally, the inhibitory effect of CB1 activation on GABA release in DGCs was reduced in epileptic animals. These morphological and physiological findings together demonstrated that the CCK-containing GABAergic inputs to the dentate gyrus were diminished in epileptic animals. These changes might play an important role in the generation of seizure in epileptic animals.

Reduced CCK immunoreactivity labeling in the inner molecular layer of the dentate gyrus

The CCK-IR, but not SOM-IR or PV-IR, in the inner molecular layer of the hippocampal dentate gyrus was diminished in the epileptic animals compared with controls. The cell count of these peptide-containing neurons has been reported, and no CCK interneuron loss was observed in our previous study (Sun et al., 2007a). The reduced CCK-IR in the inner molecular layer was also reported in this animal model (Schwarzer et al., 1995) and after kainic acid injection previously (Fredens et al., 1987). It was also reported that the CCK content of the active epileptic spiking cortex was significantly decreased in comparison to electrographically epileptic spike free lateral temporal cortex in patients (Iadarola & Sherwin, 1991). However, the mRNA of CCK expression was increased in TLE patients and animal models (Gruber et al., 1993; Iadarola & Sherwin, 1991; Schwarzer et al., 1995). These studies suggest that synthesis or processing of CCK polypeptide from the mRNA is inhibited in epileptic animals. There was a down-regulation of CCK-IR in the mossy fiber system of kainic acid-treated mice (Arabadzisz et al., 2005; Gall, 1988), but this was not found in rats (Fredens et al., 1987; Greenwood et al., 1981). The distribution of CCK-IR in our study in control animals was similar to that described in previous studies in rats. The CCK antibody was characterized before data were collected, and no background staining was found. Our result suggested that decreased concentration of CCK in afferent and efferent fibers of the hippocampus, or that there is loss of CCK immunoreactivity. CCK-IR in the inner molecular layer of the dentate gyrus may be contained in commissural associational fibers, in fibers arising from basket cells of the dentate gyrus, from fibers of the perforant path expressing CCK, or dendrites of CCK-IR interneurons (Fredens et al., 1987; Greenwood et al., 1981; Leranth & Frotscher, 1986).

Reduced α2 immunoreactive labeling in the inner molecular layer of the dentate gyrus

The α2 subunit-IR in the inner molecular layer was also reduced in epileptic animals. CCK-IR cells influence their target pyramidal cells by GABA acting via $GABA_A$ receptors

enriched in α2 subunits (Nyíri G. et al., 2001) that are known to mediate the anxiolytic effects of benzodiazepines. They also release CCK, which has anxiogenic effects via CCK_2 receptors (Freund & Katona, 2007; Sun et al., 2007a). Our finding further confirmed the close relationship between CCK-containing interneurons and α2 subunit-containing GABA receptors in the dentate gyrus. A similar finding was reported in a previous study, in which the α2 subunit-IR in both the molecular and granule cell layers of the dentate gyrus was significantly reduced in antiepileptic drug resistant rats in an animal model of TLE (Bethmann et al., 2008); however, the inner molecular layer was not discriminated from the whole dentate gyrus. A significant reduction of the α2 subunit mRNA in the granule cell layer was found in an electrical stimulation model (Nishimura et al., 2005). In an amygdala stimulation model, the mRNA of α2 subunit in the dentate gyrus was decreased by approximately 10 % in epileptic animals compared with controls (Laurén H.B. et al., 2003). In contrast to these findings, the α2 subunit-IR (Schwarzer et al., 1997), but not mRNA (Schwarzer et al., 1997) was increased in the molecular layer of the dentate gyrus 30 days after kainic acid injection and in TLE patients. The differences might be due to the differences in models, species, or methods.

CCK symmetric synapses were reduced, but not the symmetric synaptic volumetric density

In epileptic animals, the number of CCK-positive symmetric synapses out of total symmetric synapses in the inner molecular layer was less than that in control animals. The CCK terminals establish symmetric synaptic contacts on the cell bodies and dendrites of dentate granule cells (Leranth & Frotscher, 1986). The reduction in the ratio of CCK-positive symmetric synapses versus the total symmetric synapses in the inner molecular layer could result from either the reduced number of GABAergic synapses made by CCK terminals and/or increased total numbers of symmetric synapses. However, the average volumetric density of symmetric synapses in the inner molecular layer was not altered in our follow-up experiment. A selective increase in the number of symmetric synapses in the pyramidal basket cells of seizure-sensitive gerbils was found compared with seizure-resistant gerbils; however, there was no difference in the number of either symmetric or asymmetric axosomatic synapses on granule cells between seizure-sensitive and resistant gerbils (Farias et al., 1992). In the dentate gyrus of epileptic humans, the amount of somatic synapses did not change significantly, whereas, the synaptic coverage of the axon initial segment was increased 3 times (Wittner et al., 2001). However, these two findings were focused on the granule cell layer, and to our knowledge, there are few studies in the inner molecular layer. Thus, diminished CCK-positive symmetric synapses in the inner molecular layer most likely reflect the loss of CCK-positive terminals in the dendritic tree.

The total number of symmetric synapses in our study would be reduced due to the reduced CCK-IR synapses if the results were corrected for the shrinkage of epileptic tissue. This method was used in a previous study and demonstrated that the dendritic inhibition in CA1 was decreased in an animal model of epilepsy after correction for shrinkage (38 %) in epileptic tissue (Cossart et al., 2001). However, we could not exclude the possibility that epileptic animals had reduced CCK neuropeptide levels at the terminals, a loss of CCK neuropeptide immunoreactivity, or a combination of both.

Analysis of Golgi-stained axonal plexuses from single basket cells indicates that they extend on an average of 400 μm in the transverse axis and 1.1 mm in the septotemporal axis. Therefore, it is conceivable that a single basket cell may influence a very large number of granule cells (Struble et al., 1978). In the hippocampus, PV-IR and CCK-IR basket cells are important in controlling synchronous network activity patterns by regulating the firing of large groups of principal cells by blocking or delaying sodium-dependent action potential generation (Cobb et al., 1995; Miles et al., 1996). There are considerable differences

between CCK and PV cells in their connectivity, expression of transmitter receptors, and their physiological properties; see reviews (Freund, 2003; Freund & Katona, 2007). Basically, the PV-IR basket cells operate as non-plastic clockwork for cortical network oscillations, whereas CCK-IR interneurons function as a sensitive, plastic fine-tuning device (Freund & Katona, 2007). Therefore, the reorganization of CCK-positive terminals in the inner molecular layer may induce the malfunction of CCK-mediated tuning and lead to abnormal rhythmic synchrony and seizure.

Functional change of CCK-containing GABAergic inputs to DGCs

Our physiological data supported the hypothesis that the loss of CCK-containing GABAergic terminals and synapses in the inner molecular layer of the dentate gyrus causes the reduction of CCK-containing GABAergic synaptic transmission to DGCs. A similar result was reported in the CA1 area (Wyeth et al., 2010). CB1 cannabinoid receptors are selectively expressed in CCK-containing basket cells and inhibit the release of GABA (Katona et al., 1999; Tsou et al., 1999). We found the inhibitory effect of a CB1 agonist was reduced in epileptic animals, which supports the loss of CCK-containing GABAergic innervations to DGCs. CCK-containing interneurons also express M1/M3 receptors on their cell bodies. The effect of M1/M3 receptor activation on GABA release was also diminished in the CA1 area, which is consistent with the loss of CCK-containing terminals (Wyeth et al., 2010).

Basket cells also differ in the voltage-gated calcium channels expressed in their terminals. The release of GABA from PV-containing basket cells is mediated by P/Q- type calcium channels, whereas from CCK-containing basket cells is mediated by N-type calcium channels (Hefft & Jonas P., 2005; Poncer et al., 1997; Wilson et al., 2001). The GABAergic inputs sensitive to the P/Q- type channel blocker were relatively increased, and the GABAergic inputs sensitive to the N-type channel blocker were decreased, which further confirmed that CCK-containing GABAergic inputs were reduced in epileptic animals. An increase in GABAergic inputs sensitive to the P/Q- type channel blocker was also reported in the CA1 area previously (Wyeth et al., 2010). Given the important inhibitory effect of CB1 receptors, the reduction of CCK-containing inputs in the inner molecular layer could contribute to the impaired balance of inhibition and excitation in the dentate gyrus. Therefore, the reduction of CCK-positive symmetric synapses in the inner molecular layer, in association with the increased excitatory input from mossy fibers (Cossart et al., 2001), would tend to reduce seizure threshold.

The reorganized CCK-containing terminals and symmetric synapses in the dentate gyrus might play important roles in epileptic animals. CCK-IR interneurons exert their effects via both GABA and CCK, and the imbalance of inhibition and excitation, as well as abnormal rhythmic synchrony, might be very important to the development and maintenance of epilepsy. A recent study suggested interneuron cell transplantation is a powerful approach to halting seizures and rescuing accompanying deficits in severely epileptic mice (Hunt et al., 2013). The novel *in vivo* optogenetic technique showed either optogenetic inhibition of excitatory principal cells, or activation of a subpopulation of GABAergic cells representing < 5 % of hippocampal neurons, stops seizures rapidly upon light application (Hunt et al., 2013; Krook-Magnuson et al., 2013). Thus, CCK-containing GABA interneurons might be good targets for a better approach to epilepsy treatment.

References

Arabadzisz D, Antal K, Parpan F, Emri Z, Fritschy JM. Epileptogenesis and chronic seizures in a mouse model of temporal lobe epilepsy are associated with distinct EEG patterns and selective

neurochemical alterations in the contralateral hippocampus. Exp Neurol. 2005; 194:76–90. [PubMed: 15899245]

Bertram EH, Williamson JM, Cornett JF, Spradlin S, Chen ZF. Design and construction of a long-term continuous video-EEG monitoring unit for simultaneous recording of multiple small animals. Brain Res Protoc. 1997; 2:85–97.

Best N, Mitchell J, Baimbridge KG, Wheal HV. Changes in parvalbumin-immunoreactive neurons in the rat hippocampus following a kainic acid lesion. Neurosci Lett. 1993; 155:1–6. [PubMed: 8361655]

Bethmann K, Fritschy JM, Brandt C, Löscher W. Antiepileptic drug resistant rats differ from drug responsive rats in GABA(A) receptor subunit expression in a model of temporal lobe epilepsy. Neurobiol Dis. 2008; 3:169–187. [PubMed: 18562204]

Buckmaster PS, Dudek FE. Neuron loss, granule cell axon reorganization, and functional changes in the dentate gyrus of epileptic kainate-treated rats. J Comp Neurol. 1997; 385:385–404. [PubMed: 9300766]

Cobb SR, Buhl EH, Halasy K, Paulsen O, Somogyi P. Synchronization of neuronal activity in hippocampus by individual GABAergic interneurons. Nature (London). 1995; 378:75–78. [PubMed: 7477292]

Commons KG, Milner TA. Localization of delta opioid receptor immunoreactivity in interneurons and pyramidal cells in the rat hippocampus. J Comp Neurol. 1997; 381:373–387. [PubMed: 9133574]

Cossart R, Dinocourt C, Hirsch JC, Merchan-Perez A, De Felipe J, Ben-Ari Y, et al. Dendritic but not somatic GABAergic inhibition is decreased in experimental epilepsy. Nat Neurosci. 2001; 4:52–62. [PubMed: 11135645]

de Lanerolle NC, Kim JH, Robbins RJ, Spencer DD. Hippocampal interneuron loss and plasticity in human temporal lobe epilepsy. Brain Res. 1989; 495:387–395. [PubMed: 2569920]

Farias PA, Low SQ, Peterson GM, Ribak CE. Morphological evidence for altered synaptic organization and structure in the hippocampal formation of seizure-sensitive gerbils. Hippocampus. 1992; 2:229–245. [PubMed: 1308187]

Fredens K, Stengaard-Pedersen K, Wallace MN. Localization of cholecystokinin in the dentate commissural-associational system of the mouse and rat. Brain Res. 1987; 401:68–78. [PubMed: 3545391]

Freund TF. Interneuron Diversity series: Rhythm and mood in perisomatic inhibition. Trends Neurosci. 2003; 26:489–495. [PubMed: 12948660]

Freund TF, Katona I. Perisomatic Inhibition. Neuron. 2007; 56:33–42. [PubMed: 17920013]

Gall C. Seizures induce dramatic and distinctly different changes in enkephalin, dynorphin, and CCK immunoreactivities in mouse hippocampal mossy fibers. J Neurosci. 1988; 8:1852–1862. [PubMed: 2898512]

Greenwood RS, Godar SE, Reaves TA, Hayward JN. Cholecystokinin in hippocampal pathways. J Comp Neurol. 1981; 203:335–350. [PubMed: 7320233]

Gruber B, Greber S, Sperk G. Kainic acid seizures cause enhanced expression of cholecystokinin-octapeptide in the cortex and hippocampus of the rat. Synapse. 1993; 15:221–228. [PubMed: 8278898]

Halasy K, Somogyi P. Subdivisions in the multiple GABAergic innervation of granule cells in the dentate gyrus of the rat hippocampus. Eur J Neurosci. 1993; 5:411–429. [PubMed: 8261118]

Heck WL, Slusarczyk A, Basaraba AM, Schweitzer L. Subcellular localization of GABA receptors in the central nervous system using post-embedding immunohistochemistry. Brain Res Protoc. 2002; 9:173–180.

Hefft S, Jonas P. Asynchronous GABA release generates long-lasting inhibition at a hippocampal interneuron-principal neuron synapse. Nat Neurosci. 2005; 8:1319–1328. [PubMed: 16158066]

Houser CR. GABA neurons in seizure disorders: a review of immunocytochemical studies. Neurochem Res. 1991; 16:295–308. [PubMed: 1780031]

Houser, CR. Interneurons of the dentate gyrus: an overview of cell types, terminal fields and neurochemical identity. In: Scharfman, Helen E., editor. Progress in Brain Research The Dentate Gyrus: A Comprehensive Guide to Structure, Function, and Clinical Implications. Elsevier; 2007. p. 217-811.

Hunt RF, Girskis KM, Rubenstein JL, Alvarez-Buylla A, Baraban SC. GABA progenitors grafted into the adult epileptic brain control seizures and abnormal behavior. Nat Neurosci. 2013; 16:692–7. [PubMed: 23644485]

Iadarola MJ, Sherwin AL. Alterations in cholecystokignin peptide and mRNA in actively epileptic human temporal cortical foci. Epilepsy Research. 1991; 8:58–63. [PubMed: 2060503]

Joshi, S.; Kapur, J. GABA(A) receptor plasticity during status epilepticus. In: Noebels, Jeffrey L.; Avoli, Massimo; Rogawski, Michael A.; Olsen, Richard W.; Delgado-Escueta, Antonio V., editors. Jasper's Basic Mechanisms of the Epilepsies. 4. Bethesda (MD): National Center for Biotechnology Information (US); 2012. p. 545-554.

Katona I, Sperlágh B, Sík A, Käfalvi A, Vizi ES, Mackie K, et al. Presynaptically located CB1 cannabinoid receptors regulate gaba release from axon terminals of specific hippocampal interneurons. J Neurosci. 1999; 19:4544–4558. [PubMed: 10341254]

Kosaka T, Hama K, Wu JY. GABAergic synaptic boutons in the granule cell layer of rat dentate gyrus. Brain Res. 1984; 293:353–359. [PubMed: 6320972]

Krook-Magnuson E, Armstrong C, Oijala M, Soltesz I. On-demand optogenetic control of spontaneous seizures in temporal lobe epilepsy. Nat Commun. 2013; 4:1376. [PubMed: 23340416]

Laurén HB, Pitkänen A, Nissinen J, Soini SL, Korpi ER, Holopainen IE. Selective changes in gamma-aminobutyric acid type A receptor subunits in the hippocampus in spontaneously seizing rats with chronic temporal lobe epilepsy. Neurosci Lett. 2003; 349:58–62. [PubMed: 12946586]

Leranth C, Frotscher M. Synaptic connections of cholecystokinin-immunoreactive neurons and terminals in the rat fascia dentata: A combined light and electron microscopic study. J Comp Neurol. 1986; 254:51–64. [PubMed: 3027137]

Lothman EW, Bertram EH, Bekenstein JW, Perlin JB. Self-sustaining limbic status epilepticus induced by continuous hippocampal stimulation: electrographic and behavioral characteristics. Epilepsy Res. 1989; 3:107–119. [PubMed: 2707248]

Maglóczky Z, Wittner L, Borhegyi Z, Halász P, Vajda J, Czirják S, et al. Changes in the distribution and connectivity of interneurons in the epileptic human dentate gyrus. Neuroscience. 2000; 96:7–25. [PubMed: 10683405]

Mangan PS, Sun C, Carpenter M, Goodkin HP, Sieghart W, Kapur J. Cultured hippocampal pyramidal neurons express two kinds of gabaa receptors. Mol Pharmacol. 2005; 67:775–788. [PubMed: 15613639]

Mathern GW, Babb TL, Leite JP, Pretorius JK, Yeoman KM, Kuhlman PA. The pathogenic and progressive features of chronic human hippocampal epilepsy. Epilepsy Res. 1996; 26:151–161. [PubMed: 8985697]

Miles R, Tóth K, Gulyás AI, Hájos N, Freund TF. Differences between somatic and dendritic inhibition in the hippocampus. Neuron. 1996; 16:815–823. [PubMed: 8607999]

Nishimura T, Schwarzer C, Gasser E, Kato N, Vezzani A, Sperk G. Altered expression of GABA(A) and GABA(B) receptor subunit mRNAs in the hippocampus after kindling and electrically induced status epilepticus. Neuroscience. 2005; 134:691–704. [PubMed: 15951123]

Nyíri G, Freund TF, Somogyi P. Input-dependent synaptic targeting of alpha(2)-subunit-containing GABA(A) receptors in synapses of hippocampal pyramidal cells of the rat. Eur J Neurosci. 2001; 13:428–442. [PubMed: 11168550]

Poncer JC, McKinney RA, Gähwiler BH, Thompson SM. Either N- or P-type calcium channels mediate gaba release at distinct hippocampal inhibitory synapses. Neuron. 1997; 18:463–472. [PubMed: 9115739]

Schwarzer C, Williamson JM, Lothman EW, Vezzani A, Sperk G. Somatostatin, neuropeptide Y, neurokinin B and cholecystokinin immunoreactivity in two chronic models of temporal lobe epilepsy. Neuroscience. 1995; 69:831–845. [PubMed: 8596652]

Schwarzer C, Tsunashima K, Wanzenböck C, Fuchs K, Sieghart W, Sperk G. GABA(A) receptor subunits in the rat hippocampus II: Altered distribution in kainic acid-induced temporal lobe epilepsy. Neuroscience. 1997; 80:1001–1017. [PubMed: 9284056]

Sloviter RS. Decreased hippocampal inhibition and a selective loss of interneurons in experimental epilepsy. Science. 1987; 235:73–76. [PubMed: 2879352]

Struble RG, Desmond NL, Levy WB. Anatomical evidence for interlamellar inhibition in the fascia dentata. Brain Res. 1978; 152:580–585. [PubMed: 687975]

Sun C, Mtchedlishvili Z, Bertram EH, Erisir A, Kapur J. Selective loss of dentate hilar interneurons contributes to reduced synaptic inhibition of granule cells in an electrical stimulation-based animal model of temporal lobe epilepsy. J Comp Neurol. 2007a; 500:876–893. [PubMed: 17177260]

Sun C, Mtchedlishvili Z, Erisir A, Kapur J. Diminished neurosteroid sensitivity of synaptic inhibition and altered location of the alpha4 subunit of GABA(A) receptors in an animal model of epilepsy. J Neurosci. 2007b; 27:12641–12650. [PubMed: 18003843]

Sun C, Sieghart W, Kapur J. Distribution of alpha1, alpha4, gamma2, and delta subunits of GABA(A) receptors in hippocampal granule cells. Brain Res. 2004; 1029:207–216. [PubMed: 15542076]

Tsou K, Mackie K, Sañudo-Peña MC, Walker JM. Cannabinoid CB1 receptors are localized primarily on cholecystokinin-containing GABAergic interneurons in the rat hippocampal formation. Neuroscience. 1999; 93:969–975. [PubMed: 10473261]

Wilson RI, Kunos G, Nicoll RA. Presynaptic specificity of endocannabinoid signaling in the hippocampus. Neuron. 2001; 31:453–462. [PubMed: 11516401]

Wittner L, Maglóczky Z, Borhegyi Z, Halász P, Tóth S, Eross L, et al. Preservation of perisomatic inhibitory input of granule cells in the epileptic human dentate gyrus. Neuroscience. 2001; 108:587–600. [PubMed: 11738496]

Wyeth MS, Zhang N, Mody I, Houser CR. Selective reduction of cholecystokinin positive basket cell innervation in a model of temporal lobe epilepsy. J Neurosci. 2010; 30:8993–9006. [PubMed: 20592220]

Research highlights

- We studied the plasticity of inputs from interneurons to the dentate gyrus in epileptic rats.
- Immunoreactivity for CCK and the α2 subunit of $GABA_A$ receptor was decreased in the inner molecular layer.
- The ratio of CCK-positive to total symmetric synapses was reduced.
- GABA release from CCK-containing interneurons was reduced.
- The inhibitory effect of CB1 receptor activation on GABA release was also reduced in epileptic rats.

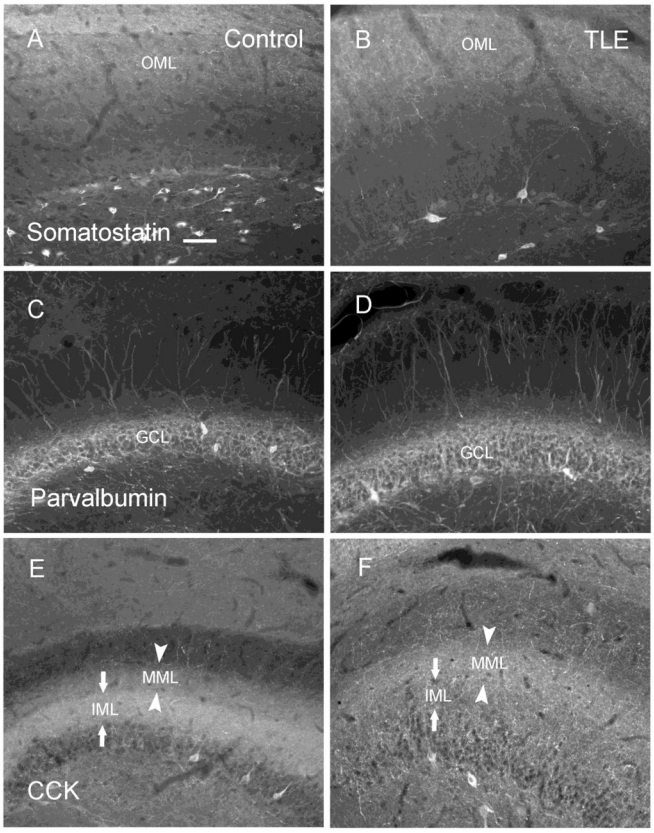

Figure 1.

The staining distribution of somatostatin (SOM), neuropeptide Y (NPY), cholecystokinin (CCK) immunoreactive (IR) fibers in the hippocampal dentate gyrus of control (A, C, E) and epileptic (B, D, F) animals. SOM-IR was mainly localized in the outer molecular layer, and its distribution was similar to that in control (A) and epileptic (B) animals. The distribution of PV-IR staining in the granule cell layer remained similar in sections from control (C) and epileptic (D) animals. CCK-IR was localized in the inner molecular layer and the middle molecular layer in controls (E), and decreased in the inner molecular layer and slightly increased in the middle molecular layer in epileptic animals (F). Scale bar in A is 60 μm. IML, inner molecular layer; MML, middle molecular layer; OML, outer molecular layer.

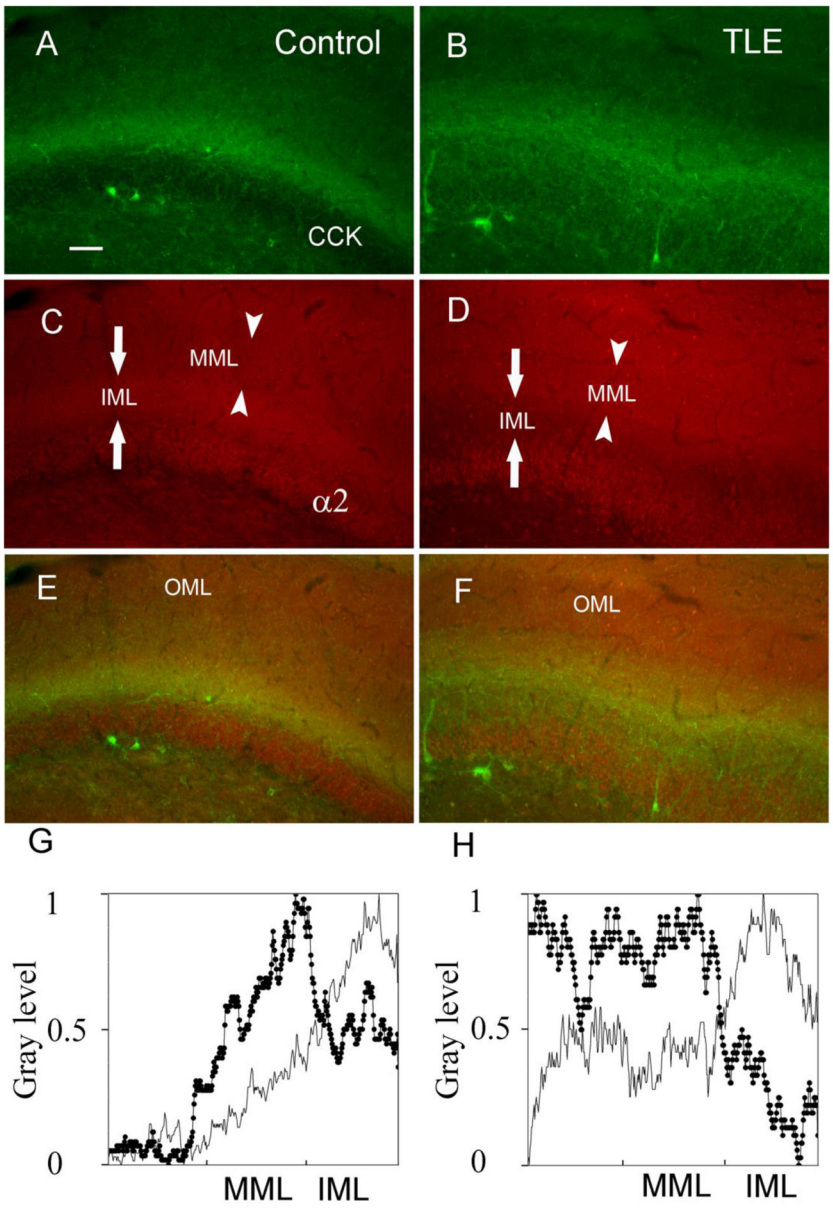

Figure 2.

Double-labeling of CCK and the α2 subunit of $GABA_A$ receptor in the hippocampal dentate gyrus in control (A, C, E) and epileptic (B, D, F) animals. The CCK (A and B) and α2 subunit-IR staining (C and D) was decreased in the inner molecular layer in epileptic animals (B and D) compared with control animals (A and C). Merged images of CCK-IR and α2 subunit-IR demonstrated that these two markers were reorganized similarly in the inner molecular layer in epileptic animals (F) compared with control animals (E). The linescan histogram of the molecular layer from control (gray line) and epileptic animals (dark line with filed circles) better demonstrated the reduced gray level of CCK (G) and α2 (H) in the inner molecular layer in epileptic animals; the relative gray level from 0 to 1 in Y axis represents no label to the brightest label. Scale bar in A is 60 μm. MML, middle molecular layer; IML, inner molecular layer; OML, outer molecular layer.

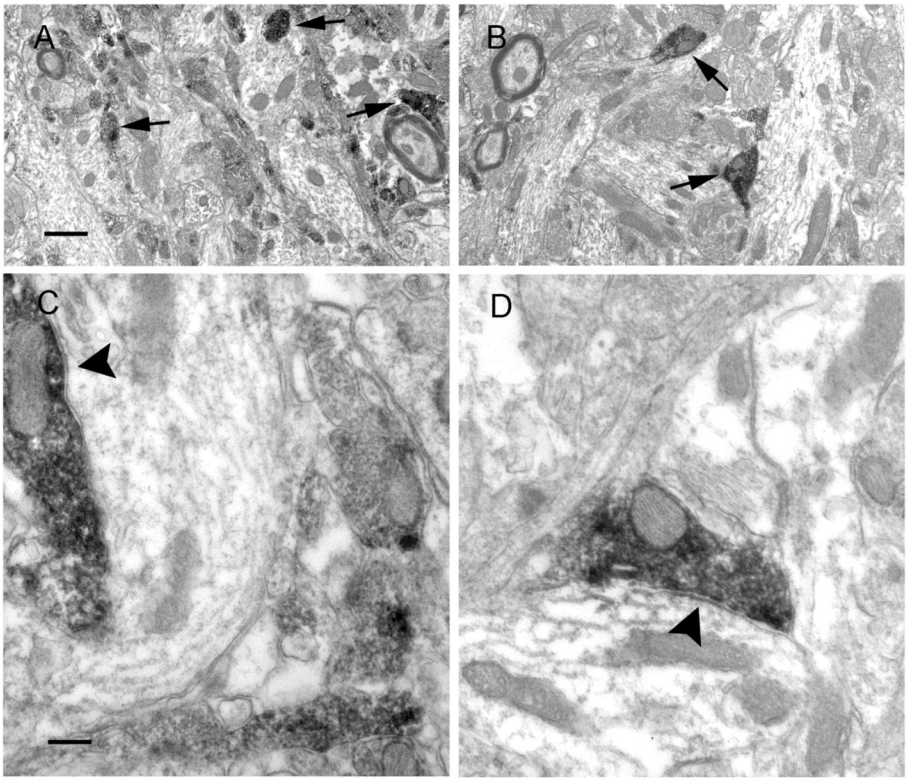

Figure 3.

Electron micrographs of CCK pre-embedding electron microscopy in the inner molecular layer of the hippocampal dentate gyrus from control (A, C) and epileptic animals (B, D). In low magnification (3k) images, DAB-labeled CCK-containing profiles were found predominately in terminals in the inner molecular layer (see arrows), and they appeared less frequently in epileptic animals (B) compared with those in control animals (A). In high magnification (8K) images, CCK terminals were found in the inner molecular layer and made symmetric synapses (see arrowheads) with dendritic shafts in sections from control (C) and epileptic animals (D). Scale bars in A and C are 500 nm and 200 nm, respectively.

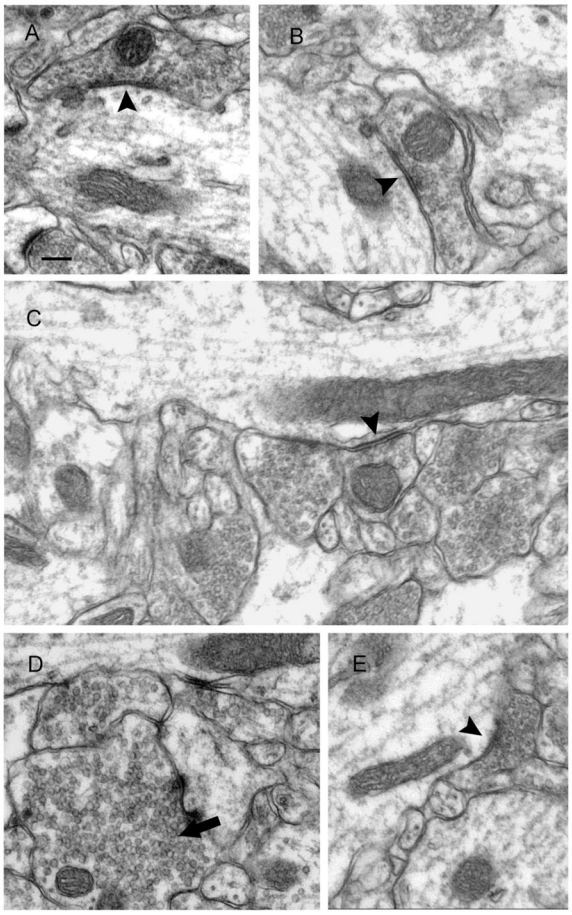

Figure 4.
Electron micrographs of the inner molecular layer from control (A and B) and epileptic animals (C–E) demonstrating that terminals made symmetric synapses with dendritic shafts (arrowheads). Dense vesicles could be found in some presynaptic terminals (C, E), which contain a certain type of neuropeptide. Mossy fibers were also found in the inner molecular layer, and they were characterized by large in size, full of round vesicles, irregular shape (D, arrow). Scale bar in A is 200 nm.

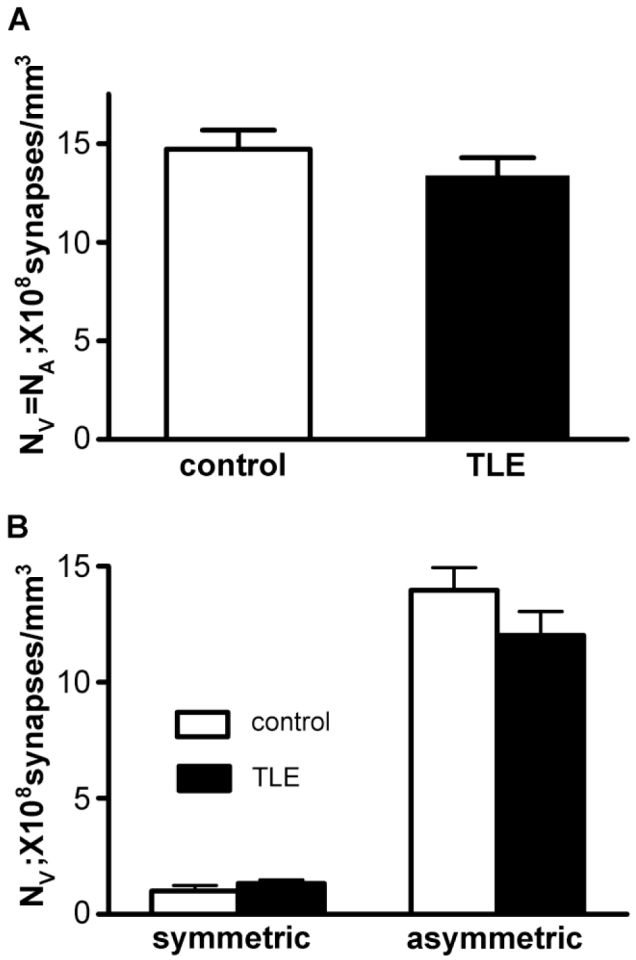

Figure 5.

Average volumetric synaptic density (N_V) in the inner molecular layer. N_v of total synapses in the inner molecular layer was similar between control and epileptic animals ($p > 0.05$) (A). The N_v of symmetric and asymmetric synapses in the inner molecular layer in epileptic animals was similar to that in control animals ($p > 0.05$) (B). For this analysis, each photograph, representing 30 - 50 μm^2 of the inner molecular layer, was used as an individual sample.

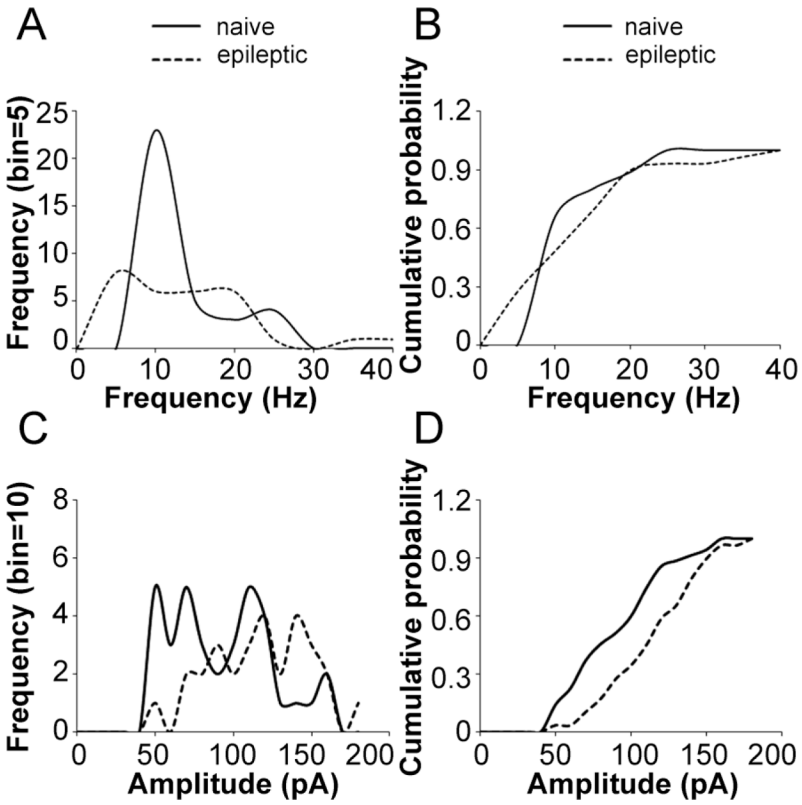

Figure 6.

The change of GABAergic current in epilepsy animals. A histogram illustrates that the distribution of sIPSC frequency had more peaks and was left-shifted (A). The cumulative distribution of sIPSC frequency was left-shifted (n = 29, $p < 0.05$) (B). A histogram illustrates that the distribution of sIPSC amplitude was right-shifted (C). The cumulative distribution of sIPSC amplitude was right-shifted (n = 29, $p < 0.01$) (D).

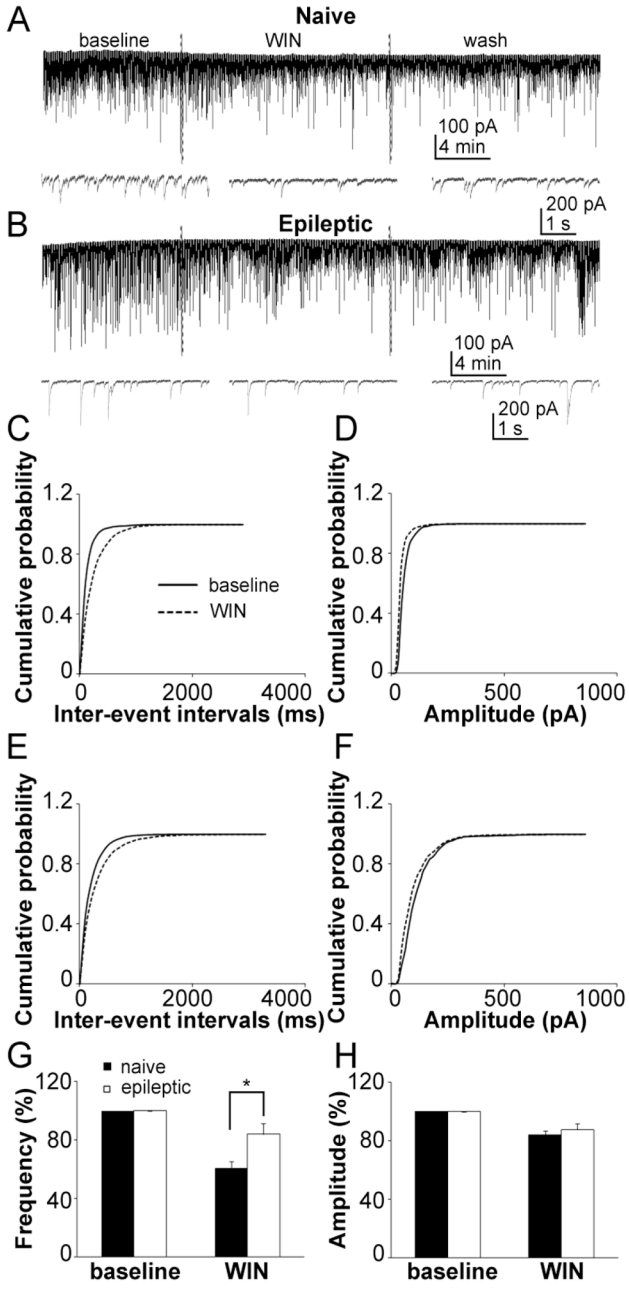

Figure 7.

The inhibitory effect of CB1 cannabinoid receptors on GABA release was reduced in epileptic animals. Representative recordings of sIPSC recording from naïve (A) and epileptic (B) rat DGCs with a 10 min baseline, 15 min application of the CB1 agonist WIN (5 μM), and 15 min of ACSF washing. Cumulative probability plots of the sIPSC inter-event intervals (C) and amplitude (D) in naïve rats (average of 7 neurons) before (continuous line) and after (dashed lines) application of WIN. Cumulative probability plots of the sIPSC inter-event intervals (E) and amplitude (F) in epileptic rats (average of 7 neurons) before (continuous line) and after (dashed lines) application of WIN. Quantification of the effect of WIN on the frequency (G) and amplitude (H) of sIPSC in naïve (filled column) and epileptic (empty column) rats (means ± SEM).

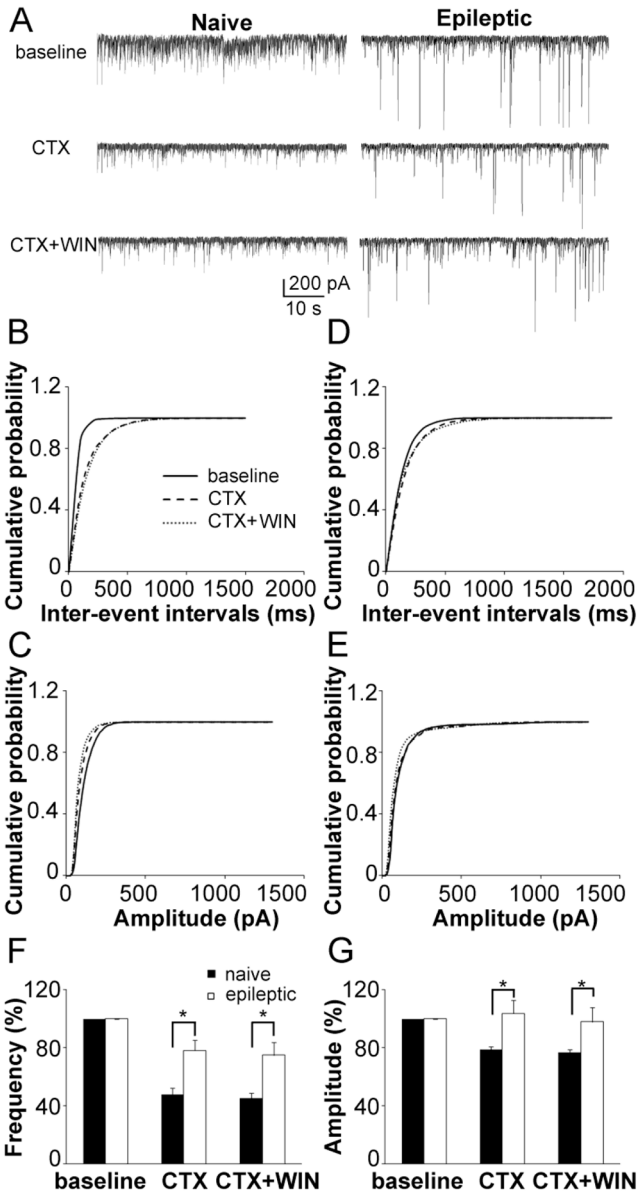

Figure 8.

The effect of N-type calcium channel blocker on GABA release was reduced in epileptic animals. Representative recording of sIPSC recording from naïve (left) and epileptic (right) rat DGCs with a 10 min baseline (up), 15 min conotoxin GVIA (CTX) application and a 15 min application of CTX with WIN (A). Cumulative probability plots of the sIPSC inter-event intervals (B) and amplitude (C) in naïve rats (average of 6 neurons) before (continuous line), and after application of CTX (larger dashed lines) and CTX with WIN (small dashed lines). Cumulative probability plots of the sIPSC inter-event intervals (D) and amplitude (E) in epileptic rats (average of 6 neurons) before (continuous line), and after application of CTX (larger dashed lines) and CTX with WIN (small dashed lines). Quantification of the effect of CTX and CTX with WIN on the frequency (F) and amplitude (G) of sIPSC in naïve (filled column) and epileptic (empty column) rats (means ± SEM).

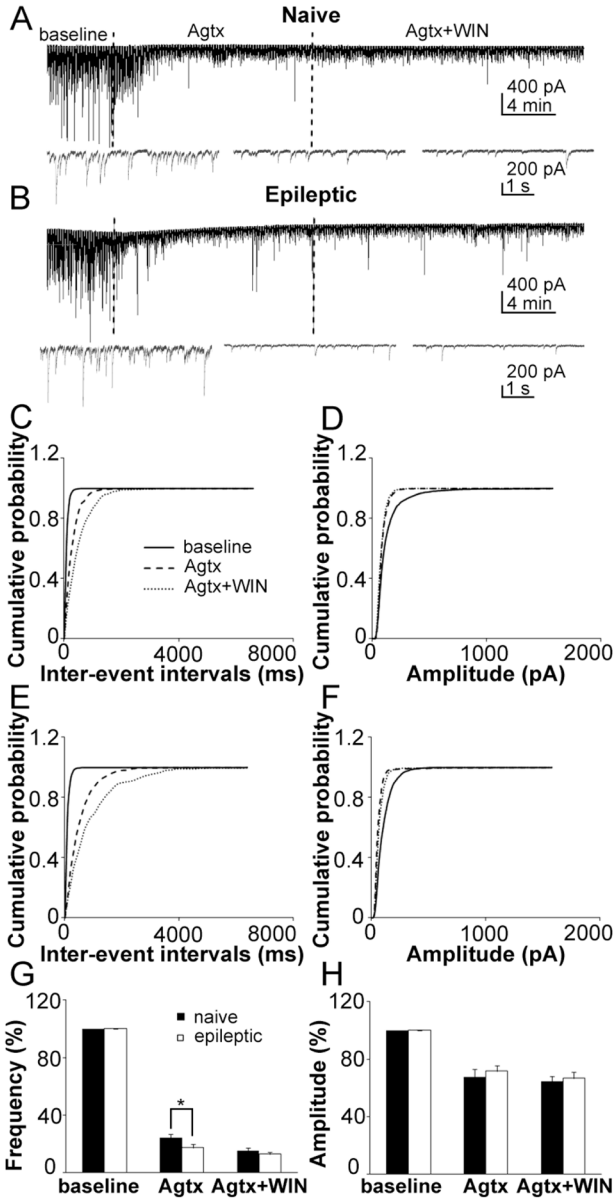

Figure 9.

The effect of P/Q-type calcium channel blocker on GABA release was increased in epileptic animals. Representative recordings of sIPSC recording from naïve (A) and epileptic (B) rat DGCs with 10 min baseline, 15 min ω-agatoxin TK (Agtx) application and 15 min Agtx with WIN. Cumulative probability plots of the sIPSC inter-event intervals (C) and amplitude (D) in naïve rats (average of 8 neurons) before (continuous line), and after application of Agtx (larger dashed lines) and Agtx with WIN (small dashed lines). Cumulative probability plots of the sIPSC inter-event intervals (E) and amplitude (F) in epileptic rats (average of 8 neurons) before (continuous line), and after application of Agtx (larger dashed lines) and CTX with WIN (small dashed lines). Quantification of the effect of Agtx and Agtx with WIN on the frequency (G) and amplitude (H) of sIPSC in naïve (filled column) and epileptic (empty column) rats (means ± SEM).

Table 1

The effect of N-type channel blocker on the frequency and amplitude of sIPSCs

	Naïve (n = 6)		Epileptic (n = 6)	
	Frequency (Hz)	**Amplitude (pA)**	**Frequency (Hz)**	**Amplitude (pA)**
Baseline	18.04 ± 2.19	118.07 ±11.68	5.00 ± 0.95	96.93 ±11.51
CTX	9.62 ±1.70**	91.75 ±10.18**	3.84 ± 0.78*	98.83 ±9.00
CTX+WIN	9.27 ±1.66	88.63 ±7.58	3.67 ±0.85	96.41 ±10.05

* $p < 0.05$,

** $p < 0.01$ (CTX vs. Baseline)

Table 2

The P/Q-type channel blocker on the frequency and amplitude of sIPSCs

	Naïve (n = 8)		Epileptic (n = 7)	
	Frequency (Hz)	**Amplitude (pA)**	**Frequency (Hz)**	**Amplitude (pA)**
Baseline	11.04 ± 0.97	120.37 ± 5.73	21.85 ± 3.70	116.40 ±8.96
CTX	2.67 ± 0.36**	80.80 ± 6.08**	4.13 ± 0.93**	82.76 ±6.63**
CTX+WIN	1.73 ± 0.25##	76.33 ±2.97	2.80 ± 0.50#	75.41 ±2.73

** $p < 0.01$ (CTX vs. Baseline);

# $p < 0.05$,

$p < 0.01$ (CTX vs. CTX+WIN)